universe

IMPACT FACTOR 2.9

CITESCORE 3.6

Article

Primordial Gravitational Wave- and Curvature Perturbation-Induced Energy Density Perturbations

Zhe Chang, Yu-Ting Kuang, Xukun Zhang and Jing-Zhi Zhou

Special Issue
Advanced Studies in Gravitational Waves

Edited by
Dr. Arnab Dasgupta

MDPI

https://doi.org/10.3390/universe10010039

universe

MDPI

Article

Primordial Gravitational Wave- and Curvature Perturbation-Induced Energy Density Perturbations

Zhe Chang [1,2,†], Yu-Ting Kuang [1,2,*], Xukun Zhang [1,2,†] and Jing-Zhi Zhou [1,2,†]

[1] Institute of High Energy Physics, Chinese Academy of Sciences, Beijing 100049, China; changz@ihep.ac.cn (Z.C.); zhangxukun@ihep.ac.cn (X.Z.); zhoujingzhi@ihep.ac.cn (J.-Z.Z.)
[2] University of Chinese Academy of Sciences, Beijing 100049, China
* Correspondence: kuangyt@ihep.ac.cn
† These authors contributed equally to this work.

Abstract: We study the second-order scalar and density perturbations generated by Gaussian curvature perturbations and primordial gravitational waves in the radiation-dominated era. After presenting all the possible second-order source terms, we obtain the explicit expressions of the kernel functions and the power spectra of the second-order scalar perturbations. We show that the primordial gravitational waves might affect second-order energy density perturbation $\delta^{(2)} = \delta\rho^{(2)}/\rho^{(0)}$ significantly. The effects of primordial gravitational waves are studied in terms of different kinds of primordial power spectra.

Keywords: primordial gravitational waves; cosmological perturbation theory; primordial power spectra

1. Introduction

The cosmological perturbations which are originated from the quantum fluctuations during inflation will inevitably induce higher-order perturbations. These induced higher-order perturbations can also affect the evolution of the universe [1].

Cosmological perturbations can be decomposed as scalar, vector, and tensor perturbations on account of the $SO(3)$ symmetry of the Friedmann–Robertson–Walker (FRW) spacetime [2–4]. Recently, the higher-order perturbations induced by the primordial perturbations have been attracting a lot of interest because of their rich phenomenology [5]. Among tensor perturbations, higher-order induced tensor perturbations are known as induced gravitational waves (GWs) [6–31]. Regarding higher-order induced scalar perturbations [32–34], a higher-order energy density perturbation $\delta^{(n)} = \rho^{(n)}/\rho^{(0)}$ can be calculated in terms of these scalar perturbations. And $\delta^{(n)}$ can affect primordial black hole (PBH) formation [35,36] and the large-scale structure (LSS) of the universe [37,38]. Higher-order induced vector perturbations can also affect many cosmological observations [5,39–48], such as redshift-space distortions [42] and weak lensing [45–47].

The source terms of high-order induced perturbations originate from the primordial perturbations generated during inflation. Since vector perturbations decay as $1/a^2$ [39], we typically neglect primordial vector perturbations. At large scales ($\geq$1 Mpc), the amplitude of a primordial scalar perturbation A_ζ is constrained by observations of the cosmic microwave background (CMB) and large-scale structures to be about $A_\zeta \simeq 2^{-9}$. For primordial tensor perturbations at large scales ($\geq$1 Mpc), the tensor-to-scalar ratio ($r = A_h/A_\zeta$) is constrained to be less than 0.06 [49], where A_h is the amplitude of the primordial tensor perturbation. Therefore, when studying higher-order induced perturbations at large scales ($\geq$1 Mpc), primordial tensor perturbations can be neglected compared with primordial scalar perturbations.

At small scales ($\leq$1 Mpc), the constraints of primordial scalar and tensor perturbations are significantly weaker than those at large scales [50]. Over the past few years, primordial scalar perturbations with large amplitude at small scales have been attracting a lot of

check for updates

Citation: Chang, Z.; Kuang, Y.-T.; Zhang, X.; Zhou, J.-Z. Primordial Gravitational Wave- and Curvature Perturbation-Induced Energy Density Perturbations. *Universe* **2024**, *10*, 39. https://doi.org/10.3390/universe10010039

Academic Editors: Arnab Dasgupta and Matteo Luca Ruggiero

Received: 12 October 2023
Revised: 15 December 2023
Accepted: 12 January 2024
Published: 14 January 2024

interest. They are closely related to primordial black holes and scalar induced GWs [51–56]. In primordial tensor perturbations at small scales, their amplitude could also be much larger than it is at large scales. Large primordial tensor perturbations at small scales can be realized using many models of early universe, such as G^2-inflation [57], spectator field [58], and so on [35]. Recently, the power spectra of second-order tensor perturbations induced by primordial scalar and tensor perturbations with large amplitudes were studied in Refs. [17,59–61]. They considered the log-normal primordial scalar and tensor power spectra at small scales and found that primordial tensor perturbations have a very important effect on second-order induced tensor perturbations.

Second-order induced scalar and energy density perturbations have been studied for many years [32–38,62]. However, a complete study of second-order induced scalar perturbations has not been presented. The importance of scalar–tensor coupling source term $\mathcal{S}_2 \sim \phi h$ has been neglected in previous studies. In this paper, we consider the second-order energy density perturbation induced by primordial curvature and tensor perturbations during the RD era systematically. Second-order scalar perturbations can be generated by scalar–scalar, scalar–tensor, and tensor–tensor coupling source terms $\mathcal{S}_1 \sim \phi\phi$, $\mathcal{S}_2 \sim \phi h$, and $\mathcal{S}_3 \sim hh$. A second-order energy density perturbation $\mathcal{P}_\delta^{(2)}$ can be calculated in terms of these second-order induced scalar perturbations. The explicit expressions of second-order scalar and energy density perturbations are presented in this work.

This paper is organized as follows: In Section 2, second-order scalar perturbations are studied. The explicit expressions of the second-order power spectra are presented. In Section 3, we investigate the second-order power spectrum in terms of monochromatic primordial power spectra. $\mathcal{P}_\delta^{(2)}$ induced by log-normal primordial power spectra are studied in Section 4. The conclusions and discussions are summarized in Section 5.

2. Second-Order Scalar Perturbations

In this section, we study the equations of motion and the kernel functions of the second-order scalar perturbations induced by primordial curvature and tensor perturbations in the RD era.

2.1. Equation of Motion

The perturbed metric in the flat FRW spacetime with Newtonian gauge is given by

$$\mathrm{d}s^2 = a^2\left[-\left(1+2\phi^{(1)}+\phi^{(2)}\right)\mathrm{d}\eta^2+\left(\left(1-2\psi^{(1)}-\psi^{(2)}\right)\delta_{ij}+h_{ij}^{(1)}\right)\mathrm{d}x^i\mathrm{d}x^j\right], \tag{1}$$

where $\phi^{(n)}$ and $\psi^{(n)}(n=1,2)$ are first-order and second-order scalar perturbations, $h_{ij}^{(1)}$ is the first-order tensor perturbation. Here, we neglect the first-order vector perturbation, since the vector modes decay as $1/a^2$ after they leave the Hubble horizon during inflation. We use the `xPand` package to study the perturbations of the Einstein equation, as `xPand` package can help us to obtain and simplify the equations of motion of cosmological perturbations [63]. The equations of motion of second-order scalar perturbations are given by

$$\Psi^{(2)}-\Phi^{(2)} = -2\Delta^{-1}\left(\partial^i\Delta^{-1}\partial^j-\frac{1}{2}\mathcal{T}^{ij}\right)\mathcal{S}_{ij}(\mathbf{x},\eta)\,, \tag{2}$$

$$\partial_\eta^2\Psi^{(2)}+3\mathcal{H}\partial_\eta\Psi^{(2)}-\frac{5}{6}\Delta\Psi^{(2)}+\mathcal{H}\partial_\eta\Phi^{(2)}+\frac{1}{2}\Delta\Phi^{(2)} = -\frac{1}{2}\mathcal{T}^{ij}\mathcal{S}_{ij}(\mathbf{x},\eta)\,, \tag{3}$$

where $\mathcal{T}^{ij}=\delta^{ij}-\partial^i\Delta^{-1}\partial^j$ is the transverse operator. During the RD era, the conformal Hubble parameter can be expressed as $\mathcal{H}=1/\eta$. For convenience, we use the symbols $\phi^{(1)}\equiv\phi$ and $h_{ij}^{(1)}\equiv h_{ij}$. As shown in Figure 1, source term $\mathcal{S}_{ij}(\mathbf{x},\eta)$ is composed of three parts: $\mathcal{S}_{ij}(\mathbf{x},\eta)=\mathcal{S}_{ij,1}+\mathcal{S}_{ij,2}+\mathcal{S}_{ij,3}$.

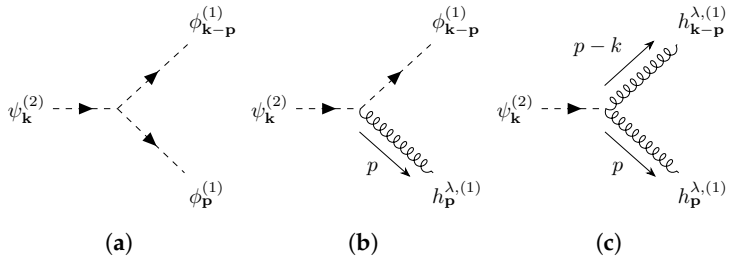

Figure 1. Source term $\mathcal{S}_{ij,1}$ is composed of the first-order scalar perturbation; source term $\mathcal{S}_{ij,2}$ is composed of the product of the first-order scalar perturbation and the first-order tensor perturbation; and source term $\mathcal{S}_{ij,3}$ is composed of the first-order tensor perturbation. (**a**) $\mathcal{S}_{ij,1} \sim \phi^{(1)}\phi^{(1)}$; (**b**) $\mathcal{S}_{ij,2} \sim \phi^{(1)}h^{\lambda,(1)}$; (**c**) $\mathcal{S}_{ij,3} \sim h^{\lambda,(1)}h^{\lambda,(1)}$.

The explicit expressions of the source terms are given in Appendix A. By substituting Equation (2) into Equation (3), we obtain the equation of motion of second-order scalar perturbation $\Psi^{(2)}$ in the RD era:

$$\begin{aligned}
&\partial_\eta^2\Psi^{(2)} + \frac{4}{\eta}\partial_\eta\Psi^{(2)} - \frac{1}{3}\Delta\Psi^{(2)} \\
&= -\frac{1}{2}\mathcal{T}^{ij}S_{ij} - 2\Delta^{-1}\left(\partial^j\Delta^{-1}\partial^i - \frac{1}{2}\mathcal{T}^{ij}\right)\left(\frac{1}{2}\Delta + \frac{1}{\eta}\partial_\eta\right)\mathcal{S}_{ij}(\mathbf{x},\eta) \\
&= \left(-\frac{1}{2}\mathcal{T}^{ij} - \left(\partial^j\Delta^{-1}\partial^i - \frac{1}{2}\mathcal{T}^{ij}\right) - 2\Delta^{-1}\left(\partial^j\Delta^{-1}\partial^i - \frac{1}{2}\mathcal{T}^{ij}\right)\frac{1}{\eta}\partial_\eta\right)S_{ij}(\mathbf{x},\eta) \\
&= -\left(\partial^j\Delta^{-1}\partial^i + 2\Delta^{-1}\left(\partial^j\Delta^{-1}\partial^i - \frac{1}{2}\mathcal{T}^{ij}\right)\frac{1}{\eta}\partial_\eta\right)\sum_{a=1}^{3}\mathcal{S}_{ij,a}(\mathbf{x},\eta)\,.
\end{aligned} \tag{4}$$

2.2. Kernel Functions

In order to solve the equation of motion of second-order scalar perturbations, we rewrite Equation (4) in momentum space as

$$\Psi^{(2)''}(\mathbf{k},\eta) + \frac{4}{\eta}\Psi^{(2)'}(\mathbf{k},\eta) + \frac{k^2}{3}\Psi^{(2)}(\mathbf{k},\eta) = \sum_{a=1}^{3}\mathcal{S}_a(\mathbf{k},\eta)\,, \tag{5}$$

where

$$\mathcal{S}_a(\mathbf{k},\eta) = \mathcal{D}_\psi^{ij}\mathcal{S}_{ij,a}(\mathbf{k},\eta)\,,\ \ \mathcal{D}_\psi^{ij} = -\left(\frac{k^ik^j}{k^2} - \left(\frac{3k^ik^j}{k^4} - \frac{\delta^{ij}}{k^2}\right)\frac{k^2}{x}\partial_x\right)\,. \tag{6}$$

Here, we have defined $x \equiv k\eta$. The explicit expressions of $\mathcal{S}_{ij,a}(\mathbf{k},\eta)(a = 1,2,3)$ are given in Appendix A. By substituting Equations (A4)–(A6) into Equation (6), we obtain the expressions of $\mathcal{S}_a(\mathbf{k},\eta)$:

$$\mathcal{S}_1 = \mathcal{D}_\psi^{ij}\mathcal{S}_{ij,1} = \int\frac{d^3p}{(2\pi)^{3/2}}k^2 f_1(u,v,x)\frac{4}{9}\zeta_{\mathbf{k-p}}\zeta_{\mathbf{p}}\,, \tag{7}$$

$$\mathcal{S}_2 = \mathcal{D}_\psi^{ij}\mathcal{S}_{ij,2} = \int\frac{d^3p}{(2\pi)^{3/2}}k^2 f_2^{\lambda_1}(u,v,x)\frac{2}{3}\zeta_{\mathbf{k-p}}\mathbf{h}_{\mathbf{p}}^{\lambda_1}\,, \tag{8}$$

$$\mathcal{S}_3 = \mathcal{D}_\psi^{ij}\mathcal{S}_{ij,3} = \int\frac{d^3p}{(2\pi)^{3/2}}k^2 f_3^{\lambda_1\lambda_2}(u,v,x)\mathbf{h}_{\mathbf{k-p}}^{\lambda_1}\mathbf{h}_{\mathbf{p}}^{\lambda_2}\,, \tag{9}$$

where λ_1 and λ_2 are the polarization indices and the spatial indices of $\mathcal{S}_{ij,a}(a = 1,2,3)$ are contracted. By substituting Equations (7)–(9) into Equation (5), we solve Equation (5) using the Green's function method:

$$\Psi^{(2)} = \sum_{a=1}^{3} \Psi_a^{(2)} \ , \ (a = 1,2,3) \ , \tag{10}$$

where

$$\Psi_1^{(2)} = \int \frac{d^3p}{(2\pi)^{3/2}} I_1(u,v,x) \frac{4}{9} \zeta_{\mathbf{k}-\mathbf{p}} \zeta_{\mathbf{p}} \ , \tag{11}$$

$$\Psi_2^{(2)} = \int \frac{d^3p}{(2\pi)^{3/2}} I_2^{\lambda_1}(u,v,x) \frac{2}{3} \zeta_{\mathbf{k}-\mathbf{p}} \mathbf{h}_{\mathbf{p}}^{\lambda_1} \ , \tag{12}$$

$$\Psi_3^{(2)} = \int \frac{d^3p}{(2\pi)^{3/2}} I_3^{\lambda_1\lambda_2}(u,v,x) \mathbf{h}_{\mathbf{k}-\mathbf{p}}^{\lambda_1} \mathbf{h}_{\mathbf{p}}^{\lambda_2} \ . \tag{13}$$

In Equations (11)–(13), the kernel functions $I_a(u,v,x)(a = 1,2,3)$ are defined as

$$\begin{aligned} I_1 &= \int_0^x \mathrm{d}\bar{x} \left(\frac{\bar{x}}{x}\right)^2 \left\{ -\frac{x\bar{x}}{\sqrt{3}} \left[j_1(x/\sqrt{3}) y_1(\bar{x}/\sqrt{3}) - j_1(\bar{x}/\sqrt{3}) y_1(x/\sqrt{3}) \right] \right\} f_1(u,v,\bar{x}) \ , \\ I_2^{\lambda_1} &= \int_0^x \mathrm{d}\bar{x} \left(\frac{\bar{x}}{x}\right)^2 \left\{ -\frac{x\bar{x}}{\sqrt{3}} \left[j_1(x/\sqrt{3}) y_1(\bar{x}/\sqrt{3}) - j_1(\bar{x}/\sqrt{3}) y_1(x/\sqrt{3}) \right] \right\} f_2^{\lambda_1}(u,v,\bar{x}) \ , \\ I_3^{\lambda_1,\lambda_2} &= \int_0^x \mathrm{d}\bar{x} \left(\frac{\bar{x}}{x}\right)^2 \left\{ -\frac{x\bar{x}}{\sqrt{3}} \left[j_1(x/\sqrt{3}) y_1(\bar{x}/\sqrt{3}) - j_1(\bar{x}/\sqrt{3}) y_1(x/\sqrt{3}) \right] \right\} f_3^{\lambda_1,\lambda_2}(u,v,\bar{x}) \ . \end{aligned} \tag{14}$$

At the end of this section, we calculate the kernel functions in Equation (14). We present these three kinds of kernel functions $(I_a(u=1,v=1,x))^2 (a = 1,2,3)$ as functions of $x = k\eta$ in Figure 2.

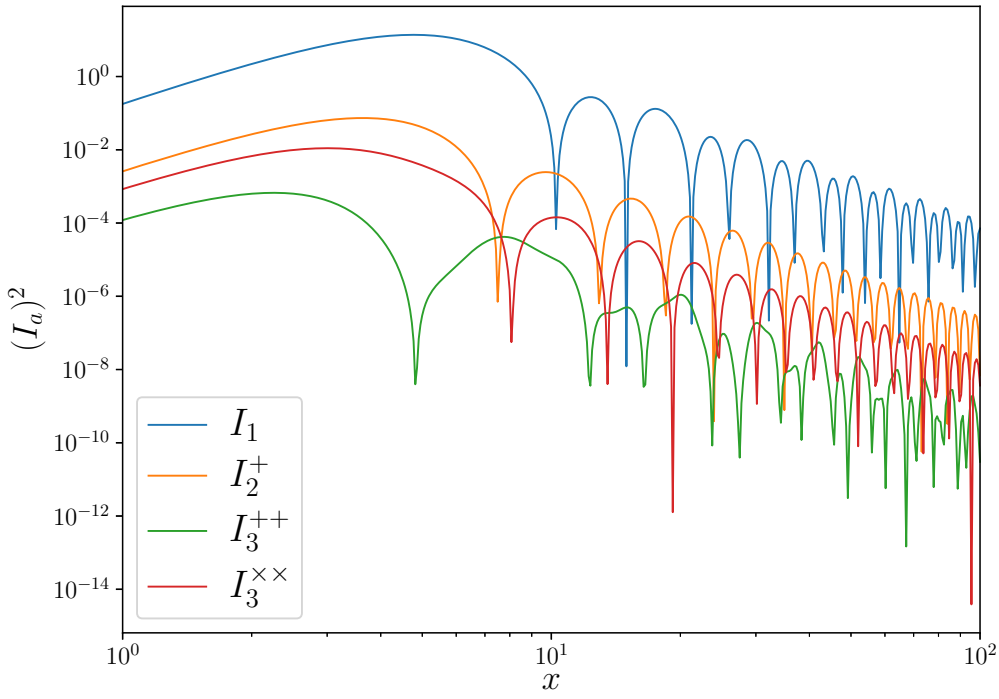

Figure 2. Kernel functions I_i $(i = 1,2,3)$ in Equation (14). We have set $u = v = 1$.

As shown in Figure 2, kernel function I_1 is much larger than other kernel functions.

2.3. Initial Second-Order Perturbation

As we mentioned in Refs. [2,32], the contributions from the initial second-order perturbation also need to be considered. More precisely, second-order scalar perturbations are composed of two parts, the second-order scalar perturbations induced by the primor-

dial perturbations and the initial second-order perturbation. The second-order curvature perturbation in the Newtonian gauge is given by [2]

$$-\zeta^{(2)} = \Psi^{(2)} + \frac{\mathcal{H}}{\rho^{(0)\prime}}\left[\delta\rho^{(2)} - \frac{\delta\rho^{(1)\prime}}{\rho^{(0)\prime}}\delta\rho^{(1)}\right] - \frac{1}{4}\chi^{k}_{\delta\rho k} + \frac{1}{4}\Delta^{-2}\partial^{i}\partial^{j}\chi_{ij\delta\rho}\,, \tag{15}$$

where

$$\begin{aligned}\chi_{ij\delta\rho} \equiv & -2\frac{\mathcal{H}}{\rho^{(0)\prime}}\left[2\mathcal{H}\left(\frac{\delta\rho^{(1)2}}{\rho^{(0)\prime}}\right) - \frac{\delta\rho^{(1)\prime}}{\rho^{(0)\prime}}\delta\rho^{(1)}\right]\delta_{ij} - \frac{2}{\rho^{(0)\prime 2}}\partial_i\delta\rho^{(1)}\partial_j\delta\rho^{(1)} \\ & + 4\left[-\frac{\delta\rho^{(1)}}{\rho^{(0)\prime}}\left[\left(-\Psi^{(1)\prime}\delta_{ij} + \frac{1}{2}h^{(1)\prime}_{ij}\right) + 2\mathcal{H}\left(-\Psi^{(1)}\delta_{ij} + \frac{1}{2}h^{(1)}_{ij}\right)\right]\right],\end{aligned} \tag{16}$$

$$\begin{aligned}\chi^{k}_{\delta\rho k} \equiv & -6\frac{\mathcal{H}}{\rho^{(0)\prime}}\left[2\mathcal{H}\left(\frac{\delta\rho^{(1)2}}{\rho^{(0)\prime}}\right) - \frac{\delta\rho^{(1)\prime}}{\rho^{(0)\prime}}\delta\rho^{(1)}\right] - \frac{2}{\rho^{(0)\prime 2}}\partial^{k}\delta\rho^{(1)}\partial_{k}\delta\rho^{(1)} \\ & + 4\left[-\frac{\delta\rho^{(1)}}{\rho^{(0)\prime}}\left[\left(-3\Psi^{(1)\prime} + \frac{1}{2}h^{(1)k\prime}_{k}\right) + 2\mathcal{H}\left(-3\Psi^{(1)} + \frac{1}{2}h^{(1)k}_{k}\right)\right]\right].\end{aligned} \tag{17}$$

In the superhorizon limit ($k\eta \ll 1$), the second-order curvature perturbation can be approximated as

$$\begin{aligned}\zeta^{(2)}(k,\eta) \simeq & \left\{-\Psi^{(2)}(k,\eta) + \frac{1}{4}\delta^{(2)} - \frac{1}{8}\delta^{(1)2} - \delta^{(1)}\Psi^{(1)}\right. \\ & \left. + \frac{\delta^{(1)}h^{(1)k}_{k}}{4} - \frac{\delta^{(1)}\nabla^{-2}\partial_i\partial_j h^{(1)ij}}{4}\right\} T_{\Psi}(k\eta)\,,\end{aligned} \tag{18}$$

where

$$\delta^{(1)} = \frac{\delta\rho^{(1)}}{\rho^{(0)}} = \frac{-6\mathcal{H}\left(\mathcal{H}\phi^{(1)} + \psi^{(1)\prime}\right) + 2\triangle\psi^{(1)}}{3\mathcal{H}^2} \simeq -2\phi^{(1)} = -\frac{4}{3}\zeta^{(1)}\,. \tag{19}$$

We assume local-type non-Gaussianity here, which is parametrized as $\zeta^{(2)} = 2a_{\rm NL}\left(\zeta^{(1)}\right)^2$ in the superhorizon limit, and $a_{\rm NL} = 1$ for Gaussian perturbations [64–66]. By substituting the condition of local-type non-Gaussianity into Equation (18), we obtain the contributions from the initial second-order perturbation:

$$\begin{aligned}\Psi^{(2)}_{\rm in}(\mathbf{k}) = & \frac{1}{3}\left(\frac{3k^ik^j}{k^4} - \frac{\delta^{ij}}{k^2}\right)\mathcal{S}_{ij} + \int\frac{d^3p}{(2\pi)^{3/2}}\left(\left(-\frac{4}{3}a_{\rm NL} + \frac{28}{27}\right)\zeta_{\mathbf{k}-\mathbf{p}}\zeta_{\mathbf{p}}\right. \\ & \left. -\frac{2}{9}\varepsilon^{\lambda,i}_{i}(\mathbf{p})\zeta_{\mathbf{k}-\mathbf{p}}\mathbf{h}^{\lambda}_{\mathbf{p}} + \frac{2}{9}\frac{p^ip^j}{p^2}\varepsilon^{\lambda}_{ij}(\mathbf{p})\zeta_{\mathbf{k}-\mathbf{p}}\mathbf{h}^{\lambda}_{\mathbf{p}}\right).\end{aligned} \tag{20}$$

After considering the effects of the initial second-order perturbation, second-order scalar perturbation $\Psi^{(2)}$ can be written as

$$\Psi^{(2)}(\mathbf{k}) = \Psi^{(2)}_{\rm in}(\mathbf{k}) + \sum_{a=1}^{3}\Psi^{(2)}_{a}\,,\ (a = 1,2,3)\,. \tag{21}$$

We study the second-order scalar and density perturbations generated by the Gaussian curvature and tensor perturbations. Therefore, we set $a_{\rm NL} = 1$ in this paper.

2.4. Power Spectra

In this section, the power spectra of second-order scalar and density perturbations are investigated. We assume that the two-point function $\langle\zeta_{\mathbf{k}_1}\mathbf{h}^{\lambda}_{\mathbf{k}_2}\rangle = 0$ for arbitrary $\mathbf{k}_1$ and $\mathbf{k}_2$ [17]. Therefore, we only need to consider three kinds of four-point functions. The explicit

expressions of these four-point functions are given in Appendix C. The power spectra of second-order scalar perturbation is defined as

$$\langle \Psi^{(2)}(\mathbf{k})\Psi^{(2)}(\mathbf{k}')\rangle = \delta(\mathbf{k}+\mathbf{k}')\frac{2\pi^2}{k^3}\mathcal{P}_\psi^{(2)} . \tag{22}$$

By substituting Equations (11)–(13) into Equation (22), we obtain

$$\langle \Psi^{(2)}(\mathbf{k})\Psi^{(2)}(\mathbf{k}')\rangle = \sum_{i=1}^{3}\langle \Psi_i^{(2)}(\mathbf{k})\Psi_i^{(2)}(\mathbf{k}')\rangle , \tag{23}$$

where

$$\begin{aligned}
\langle \Psi_1^{(2)}(\mathbf{k})\Psi_1^{(2)}(\mathbf{k}')\rangle &= \int \frac{d^3p}{(2\pi)^{3/2}}\frac{d^3p'}{(2\pi)^{3/2}} I_1(|\mathbf{k}-\mathbf{p}|,p,\eta) I_1(|\mathbf{k}'-\mathbf{p}'|,p',\eta) \\
&\quad \times \frac{16}{81}\langle \zeta_{\mathbf{k}-\mathbf{p}}\zeta_{\mathbf{p}}\zeta_{\mathbf{k}'-\mathbf{p}'}\zeta_{\mathbf{p}'}\rangle , \qquad (24)\\
\langle \Psi_2^{(2)}(\mathbf{k})\Psi_2^{(2)}(\mathbf{k}')\rangle &= \int \frac{d^3p}{(2\pi)^{3/2}}\frac{d^3p'}{(2\pi)^{3/2}} I_2^{\lambda_1}(|\mathbf{k}-\mathbf{p}|,p,\eta) I_2^{\lambda_1'}(|\mathbf{k}'-\mathbf{p}'|,p',\eta) \\
&\quad \times \frac{4}{9}\langle \zeta_{\mathbf{k}-\mathbf{p}}\mathbf{h}_{\mathbf{p}}^{\lambda_1}\zeta_{\mathbf{k}'-\mathbf{p}'}\mathbf{h}_{\mathbf{p}'}^{\lambda_1'}\rangle , \qquad (25)\\
\langle \Psi_3^{(2)}(\mathbf{k})\Psi_3^{(2)}(\mathbf{k}')\rangle &= \int \frac{d^3p}{(2\pi)^{3/2}}\frac{d^3p'}{(2\pi)^{3/2}} I_3^{\lambda_1\lambda_2}(|\mathbf{k}-\mathbf{p}|,p,\eta) I_3^{\lambda_1'\lambda_2'}(|\mathbf{k}'-\mathbf{p}'|,p',\eta) \\
&\quad \times \langle \mathbf{h}_{\mathbf{k}-\mathbf{p}}^{\lambda_1}\mathbf{h}_{\mathbf{p}}^{\lambda_2}\mathbf{h}_{\mathbf{k}'-\mathbf{p}'}^{\lambda_1'}\mathbf{h}_{\mathbf{p}'}^{\lambda_2'}\rangle . \qquad (26)
\end{aligned}$$

The corresponding Feynman diagrams of these three kinds of two-point functions are given in Figure 3.

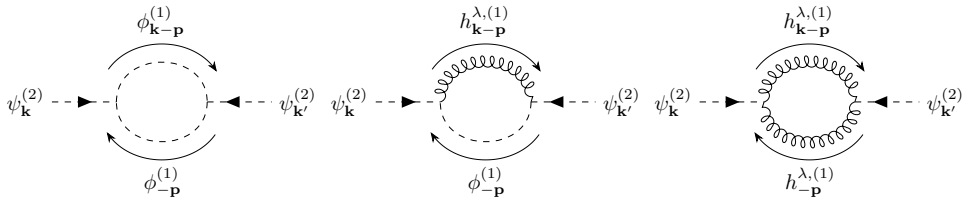

Figure 3. The Feynman diagrams of three kinds of two-point functions. (**a**) $\mathcal{P}_1^{(2)} \sim \langle \Psi_1^{(2)}(\mathbf{k})\Psi_1^{(2)}(\mathbf{k}')\rangle$; (**b**) $\mathcal{P}_2^{(2)} \sim \langle \Psi_2^{(2)}(\mathbf{k})\Psi_2^{(2)}(\mathbf{k}')\rangle$; (**c**) $\mathcal{P}_3^{(2)} \sim \langle \Psi_3^{(2)}(\mathbf{k})\Psi_3^{(2)}(\mathbf{k}')\rangle$.

By substituting Equations (A15)–(A17) into Equations (24)–(26), we obtain the explicit expressions of the power spectra:

$$\mathcal{P}_\psi^{(2)} = \mathcal{P}_1^{(2)} + \mathcal{P}_2^{(2)} + \mathcal{P}_3^{(2)} , \tag{27}$$

where

$$\begin{aligned}
\mathcal{P}_1^{(2)} &= \frac{1}{2}\int_0^\infty dv \int_{|1-v|}^{|1+v|}\frac{du}{v^2u^2} I_1(u,v,x)\mathcal{P}_\zeta(uk)\mathcal{P}_\zeta(vk) \\
&\quad \times \frac{16}{81}\Big[I_1(|\mathbf{k}'-\mathbf{p}'|,p',\eta)\big|_{\mathbf{p}'=-\mathbf{p}} + I_1(|\mathbf{k}'-\mathbf{p}'|,p',\eta)\big|_{\mathbf{p}'=\mathbf{p}-\mathbf{k}}\Big]\Big|_{\mathbf{k}'\to-\mathbf{k}} , \qquad (28)\\
\mathcal{P}_2^{(2)} &= \frac{1}{2}\int_0^\infty dv \int_{|1-v|}^{|1+v|}\frac{du}{v^2u^2} I_2^{\lambda_1}(u,v,x)\delta^{\lambda_1\lambda_1'}\mathcal{P}_\zeta(uk)\mathcal{P}_h(vk) \\
&\quad \times \frac{4}{9} I_2^{\lambda_1'}(|\mathbf{k}'-\mathbf{p}'|,p',\eta)\big|_{\mathbf{p}'=-\mathbf{p},\,\mathbf{k}'=-\mathbf{k}} , \qquad (29)
\end{aligned}$$

$$\mathcal{P}_3^{(2)} = \frac{1}{2}\int_0^\infty dv \int_{|1-v|}^{|1+v|} \frac{du}{v^2u^2} I_3^{\lambda_1\lambda_2}(u,v,x)\mathcal{P}_h(uk)\mathcal{P}_h(vk) \times \Big[\delta^{\lambda_1\lambda_1'}\delta^{\lambda_2\lambda_1'} I_3^{\lambda_1'\lambda_2'}\big(|\mathbf{k}'-\mathbf{p}'|,p',\eta\big)\big|_{\mathbf{p}'=-\mathbf{p}} + \delta^{\lambda_1\lambda_2'}\delta^{\lambda_2\lambda_1'} I_3^{\lambda_1'\lambda_2'}\big(|\mathbf{k}'-\mathbf{p}'|,p',\eta\big)\big|_{\mathbf{p}'=\mathbf{p}-\mathbf{k}}\Big]\Big|_{\mathbf{k}'=-\mathbf{k}} . \quad (30)$$

In Equations (28)–(30), the substitutions of $\mathbf{k}'$ and $\mathbf{p}'$ come from the three-dimensional delta functions in the Wick's expansions of four-point functions. Since we have assumed that the two-point function $\langle \zeta_{\mathbf{k}_1}\mathbf{h}^\lambda_{\mathbf{k}_2}\rangle = 0$, three kinds of source terms in Equations (A1)–(A3) are decoupled. More precisely, the two-point functions $\langle \Psi_i^{(2)}(\mathbf{k})\Psi_j^{(2)}(\mathbf{k}')\rangle = 0$ if $i \neq j$. As shown in Equations (28)–(30), the power spectra of second-order scalar perturbations are composed of three parts, which come from source terms $\mathcal{S}_1 \sim \phi\phi$, $\mathcal{S}_2 \sim \phi h$, and $\mathcal{S}_3 \sim hh$, respectively.

The energy density perturbation can be calculated as

$$\delta^{(2)} = \frac{\delta\rho^{(2)}}{\rho^{(0)}} = -\frac{1}{3\mathcal{H}^4}\left(\frac{1}{4}\mathcal{H}^2 h'_{ij}\left(h'^{ij} + 8\mathcal{H}h^{ij}\right) + 6\mathcal{H}^4\left(-4\phi^2 + \Phi^{(2)}\right) + 6\mathcal{H}^3\Psi^{(2)\prime} + 4\mathcal{H}\partial_i\phi'\partial^i\phi + 2\partial_i\phi'\partial^i\phi' + \mathcal{H}^2\left(-2\left(3\phi'^2 + 8\phi\Delta\phi + \Delta\Psi^{(2)} + 2\partial_i\phi\partial^i\phi + \frac{1}{2}h^{ij}\left(-\partial_i\partial_j\phi + \Delta h_{ij}\right)\right)\right.\right. + \left.\left.\frac{1}{4}\left(2\partial_l h_{ij} - 3\partial_j h_{il}\right)\partial^j h^{il}\right)\right) . \quad (31)$$

The power spectrum of second-order energy density perturbation $\mathcal{P}_\delta^{(2)}$ is defined by

$$\langle \delta^{(2)}(\mathbf{k})\delta^{(2)}(\mathbf{k}')\rangle = \delta(\mathbf{k}+\mathbf{k}')\frac{2\pi^2}{k^3}\mathcal{P}_\delta^{(2)} , \quad (32)$$

where the energy density ($\delta^{(2)}$) can be calculated in terms of Equation (21) and Equation (31).

3. Monochromatic Primordial Power Spectra

As mentioned, the constraints of primordial curvature and tensor perturbations at small scales are significantly weaker than those at large scales; the tensor-to-scalar ratio (r) can be very large at small scales. Therefore, we start with a toy model of a δ-peak. In this case, the primordial scalar and tensor perturbations are very large at small scale. Since we consider the second-order scalar and density perturbations generated by the Gaussian curvature and tensor perturbations, we have set $a_{\rm NL} = 1$ in Equation (20).

3.1. Monochromatic Primordial Power Spectra with the Same k_*

We consider monochromatic primordial power spectra, namely,

$$\mathcal{P}_\zeta = A_\zeta k_{\zeta*}\delta(k-k_{\zeta*}) , \ \mathcal{P}_h = A_h k_{h*}\delta(k-k_{h*}) , \ k_{\zeta*} = k_{h*} = k_* , \quad (33)$$

where k_* is the wavenumber at which the power spectrum has a δ-function peak. In Figure 4, we plot the three kinds of power spectra for second-order perturbations $\Phi^{(2)}$, $\Psi^{(2)}$, and $\delta^{(2)}$. Here, we use the symbols $\mathcal{P}_1^{(2)}$, $\mathcal{P}_2^{(2)}$, and $\mathcal{P}_3^{(2)}$ to represent the contributions of source terms $\mathcal{S}_1 \sim \phi\phi$, $\mathcal{S}_2 \sim \phi h$, and $\mathcal{S}_3 \sim hh$, respectively. As shown in Figure 4, for tensor-to-scalar ratio $r = A_h/A_\zeta = 1$, the second-order perturbations sourced by $\mathcal{S}_1 \sim \phi\phi$ dominate the total power spectra of $\Phi^{(2)}$, $\Psi^{(2)}$, and $\delta^{(2)}$.

In order to study the effects of the large tensor-to-scalar ratio ($r = A_h/A_\zeta$) at small scales, we calculate the total power spectra of $\Phi^{(2)}$, $\Psi^{(2)}$, and $\delta^{(2)}$ for different $r = A_h/A_\zeta$. In Figure 5, the total power spectra of second-order scalar perturbations for different r are presented. For tensor-to-scalar ratio $r \ll 1$, the effects of primordial tensor perturbations

become negligible, and the total power spectra $\mathcal{P}_\phi^{(2)}$, $\mathcal{P}_\psi^{(2)}$, and $\mathcal{P}_\delta^{(2)}$ reduce to the results in Ref. [32]. For $r \gg 1$ at small scales, the effects of primordial tensor perturbations become obvious, and the total power spectra reduce to the results in Refs. [35,37,38].

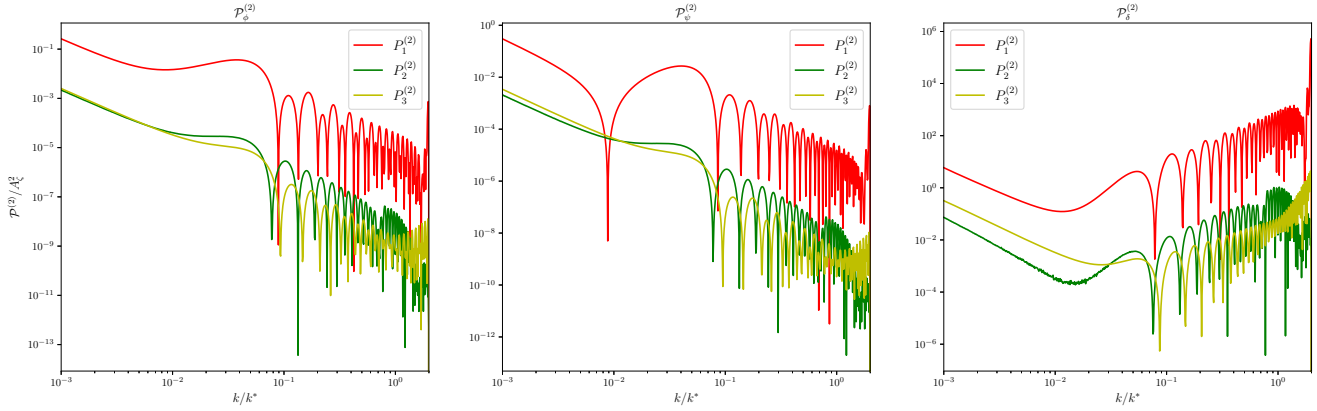

Figure 4. The three kinds of power spectra $\mathcal{P}_a^{(2)}(a = 1, 2, 3)$ for second-order perturbations $\Phi^{(2)}$, $\Psi^{(2)}$, and $\delta^{(2)}$. Power spectra $\mathcal{P}_1^{(2)}$, $\mathcal{P}_2^{(2)}$, and $\mathcal{P}_3^{(2)}$ come from source terms $\mathcal{S}_1 \sim \phi\phi$, $\mathcal{S}_2 \sim \phi h$, and $\mathcal{S}_3 \sim hh$, respectively. We have set tensor-to-scalar ratio $r = A_h/A_\zeta = 1$ and $x_* = k_*\eta = 100$.

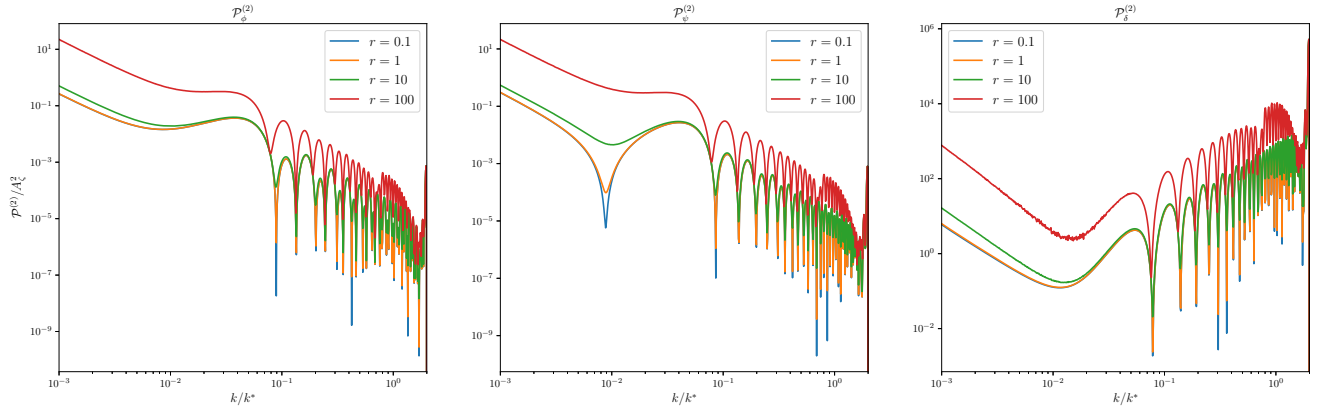

Figure 5. The total power spectra of second-order perturbations $\Phi^{(2)}$, $\Psi^{(2)}$, and $\delta^{(2)}$ for different tensor-to-scalar ratios $r = A_h/A_\zeta$. We have set $x_* = k_*\eta = 100$.

3.2. Monochromatic Primordial Power Spectra with Different k_*

The monochromatic primordial power spectra with different k_* can be written as

$$\mathcal{P}_\zeta = A_\zeta k_{\zeta*}\delta(k - k_{\zeta*}) \,, \; \mathcal{P}_h = A_h k_{h*}\delta(k - k_{h*}) \,, \; k_{\zeta*} = k_* \neq k_{h*} \,. \tag{34}$$

In Figure 6, we plot the three kinds of power spectra $\mathcal{P}_a^{(2)}(a = 1, 2, 3)$ in Equations (28)–(30) for second-order energy density perturbation $\delta^{(2)} = \delta\rho^{(2)}/\rho^{(0)}$ with different k_{h*}.

As shown in Figure 6, for $k_{h*} \neq k_{\zeta*}$, the behaviors of power spectrum $\mathcal{P}_2^{(2)}$ sourced by $\mathcal{S}_2 \sim \phi h$ are different from the case of $k_{h*}/k_{\zeta*} = 1$. More precisely, for $k_{h*}/k_{\zeta*} = n > 1$, the domain of definition of $\mathcal{P}_2^{(2)}$ is $[(n-1)k/k_*, (n+1)k/k_*]$. For $k_{h*}/k_{\zeta*} = n \gg 1$, power spectrum $\mathcal{P}_2^{(2)}$ becomes a small peak near $n \times k/k_*$. In this case, the contributions of power spectrum $\mathcal{P}_2^{(2)}$ can be neglected. And for $k_{h*}/k_{\zeta*} = n < 1$, the domain of definition of $\mathcal{P}_2^{(2)}$ is $[(1-n)k/k_*, (1+n)k/k_*]$. For $k_{h*}/k_{\zeta*} = n \ll 1$, power spectrum $\mathcal{P}_2^{(2)}$ sourced by $\mathcal{S}_2 \sim \phi h$ becomes a large peak near k/k_*.

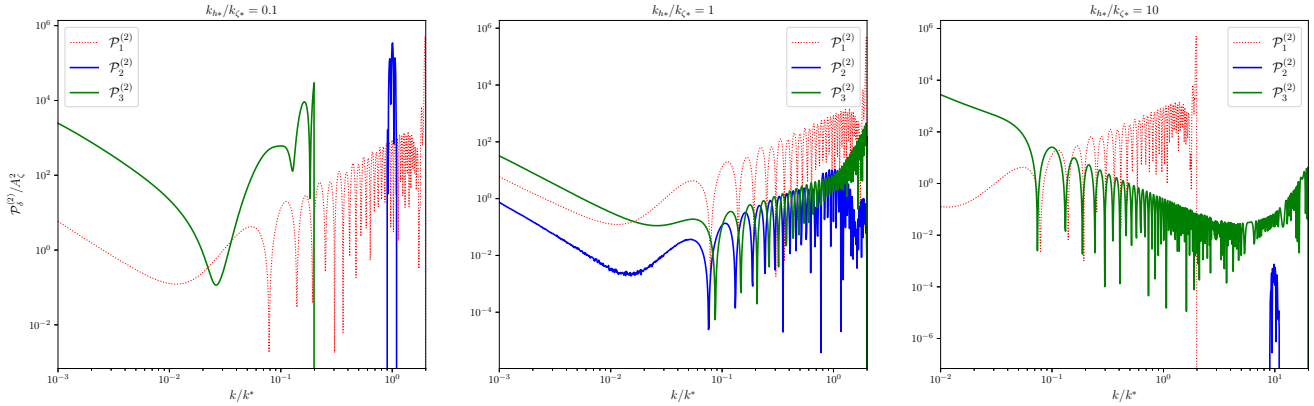

Figure 6. The power spectra $\mathcal{P}_a^{(2)}(a = 1, 2, 3)$ for second-order energy density perturbation $\delta^{(2)}$ with $k_{h*}/k_{\zeta*} = 0.1$, $k_{h*}/k_{\zeta*} = 1$, and $k_{h*}/k_{\zeta*} = 10$, respectively. We have set tensor-to-scalar ratio $r = A_h/A_\zeta = 10$, $k_{\zeta*} = k_*$, and $x_* = k_*\eta = 100$.

As shown in Figure 7, for $k_{h*}/k_{\zeta*} = 0.1$, power spectrum $\mathcal{P}_2^{(2)}$ can be larger than $\mathcal{P}_1^{(2)}$ sourced by $\mathcal{S}_1 \sim \phi\phi$, even in the case of $r = 0.1$. Note that the contributions of source term $\mathcal{S}_2 \sim \phi h$ in Equation (A2) are completely neglected in previous studies [32,35,37]. Here, we point out that the contributions of source term $\mathcal{S}_2 \sim \phi h$ are very important for the monochromatic primordial power spectra with $k_{h*}/k_{\zeta*} \ll 1$.

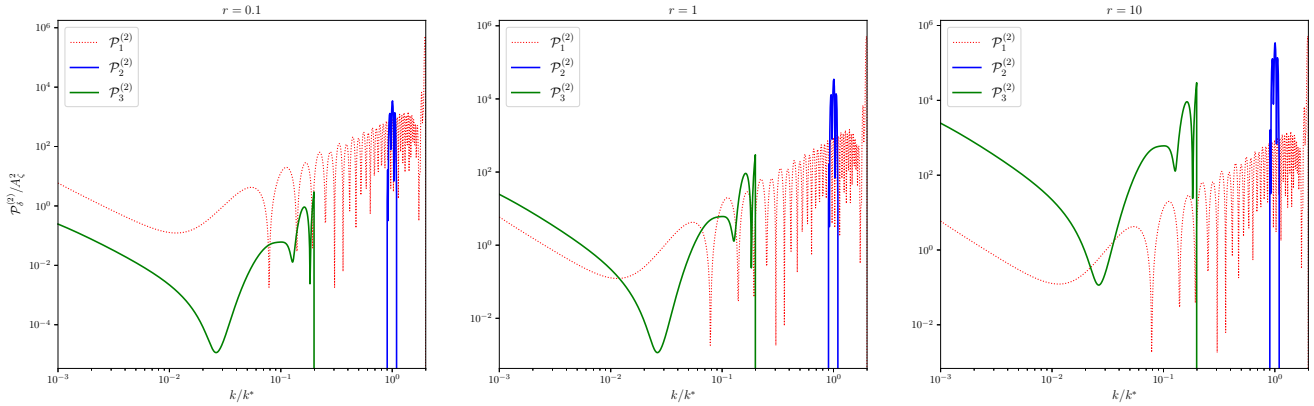

Figure 7. The power spectra $\mathcal{P}_a^{(2)}(a = 1, 2, 3)$ for second-order energy density perturbation $\delta^{(2)}$ with $r = 0.1$, $r = 1$, and $r = 10$, respectively. We have set $n = k_{h*}/k_{\zeta*} = 0.1$, $k_{\zeta*} = k_*$, and $x_* = k_*\eta = 100$.

4. Log-Normal Primordial Power Spectra

Since monochromatic primordial power spectra have infinitesimal width, it is necessary to consider a more realistic model, such as log-normal primordial power spectra. We consider the log-normal power spectra for primordial scalar and tensor perturbations. Here, we concentrated on the effects of source term $\mathcal{S}_2 \sim \phi h$ and the corresponding second-order power spectra, $\mathcal{P}_2^{(2)}$. The log-normal primordial power spectra are given by

$$\mathcal{P}_\zeta = \frac{A_\zeta}{\sqrt{2\pi\sigma_*^2}} \exp\left(-\frac{\ln^2\left(\frac{k}{k_{\zeta*}}\right)}{2\sigma_*^2}\right), \quad \mathcal{P}_h = \frac{A_h}{\sqrt{2\pi\sigma_*^2}} \exp\left(-\frac{\ln^2\left(\frac{k}{k_{h*}}\right)}{2\sigma_*^2}\right). \tag{35}$$

Here, we concentrate on the large peak of $\mathcal{P}_2^{(2)}$ with $k_{h*}/k_{\zeta*} \ll 1$. As mentioned in Section 3.2, for $k_{h*}/k_{\zeta*} = n \ll 1$, power spectrum $\mathcal{P}_2^{(2)}$ sourced by $\mathcal{S}_2 \sim \phi h$ has a large peak near $k/k_* \simeq$. For the log-normal primordial power spectra, we calculate the power spectra of second-order density perturbation $\delta^{(2)}$ with $k_{h*}/k_{\zeta*} = 0.1$. As shown in Figure 8,

for log-normal primordial power spectra, the peak of $\mathcal{P}_2^{(2)}$ becomes larger during the process of $\sigma_* \to 0$.

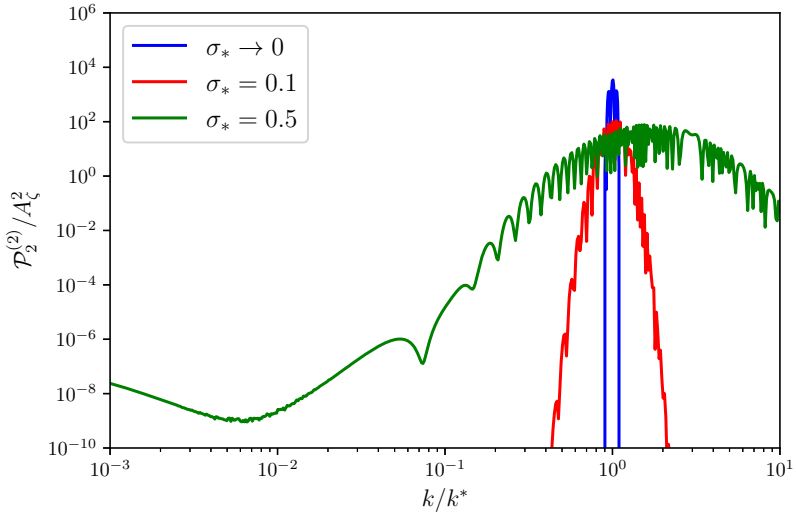

Figure 8. Power spectra $\mathcal{P}_2^{(2)}$ sourced by $\mathcal{S}_2 \sim \phi h$ for second-order energy density perturbation $\delta^{(2)}$ with $r = 0.1$. We have set $n = k_{h*}/k_{\zeta *} = 0.1$ and $x_* = k_*\eta = 100$.

For comparison, we plot $\mathcal{P}_1^{(2)}$ and $\mathcal{P}_2^{(2)}$ for second-order density perturbation $\delta^{(2)}$ with tensor-to-scalar ratio $r = 0.1$ in Figure 9. The figure shows that the contributions of $\mathcal{P}_2^{(2)}$ become smaller when σ_* increases. Namely, the effects of source term $\mathcal{S}_2 \sim \phi h$ become more obvious when σ_* and n become smaller.

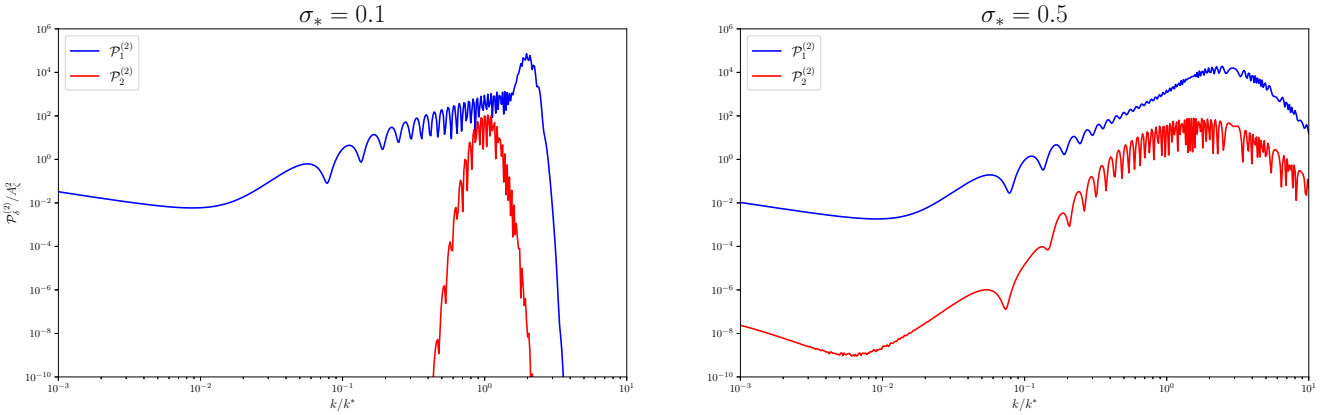

Figure 9. Power spectra $\mathcal{P}_1^{(2)}$ and $\mathcal{P}_2^{(2)}$ for second-order energy density perturbation $\delta^{(2)}$ with $r = 0.1$ for different σ_*. We have set $n = k_{h*}/k_{\zeta *} = 0.1$ and $x_* = k_*\eta = 100$.

5. Conclusions and Discussion

In this paper, we systematically studied second-order density perturbations induced by primordial gravitational waves and primordial scalar perturbations. Since the constraints of primordial curvature and tensor perturbations at small scales are significantly weaker than those at large scales, we considered large tensor-to-scalar ratios (r) at small scales. As shown in Figure 5, the effects of primordial tensor perturbations become obvious for $r \gg 1$. For tensor-to-scalar ratios $r \ll 1$, the effects of primordial tensor perturbations become negligible, and our results of power spectra $\mathcal{P}_\phi^{(2)}$, $\mathcal{P}_\psi^{(2)}$, and $\mathcal{P}_\delta^{(2)}$ reduce to the previous results in Ref. [32].

We give the explicit expressions for the power spectra of primordial scalar and tensor induced scalar and density perturbations in Equations (28)–(32). Specifically, for a given primordial scalar and tensor power spectra, the power spectra of second-order induced

scalar and density perturbations can be calculated using these equations. In this paper, we considered the primordial power spectra following delta and log-normal at small scales. It is essential to explore more general forms of primordial power spectra, such as log-normal primordial scalar power spectra and power-law primordial tensor power spectra [67].

Moreover, the second-order induced density perturbations offer a window to understand small-scale primordial gravitational waves and primordial curvature perturbations. More precisely, primordial scalar and tensor power spectra can be calculated in terms of a given inflation model. Using Equations (28)–(32), we can calculate the power spectra of second-order induced scalar and energy density perturbations. The induced density perturbations will affect many physical processes at small scales, such as the formation of PBH [68] and high-order GW background [59]. By observing PBHs or higher-order GWs, we can constrain the power spectra of second-order induced density perturbations, thereby constraining inflationary models and the physical properties of primordial scalar and gravitational waves at small scales. Related research might be given in future work.

Author Contributions: Formal analysis, Z.C., Y.-T.K., X.Z. and J.-Z.Z.; Writing—original draft, Y.-T.K. and X.Z.; Writing—review and editing, J.-Z.Z.; Supervision, Z.C. All authors have read and agreed to the published version of the manuscript.

Funding: This research was funded by the National Nature Science Foundation of China under grants No. 12075249 and 11690022 and the Key Research Program of the Chinese Academy of Sciences under grant No. XDPB15.

Data Availability Statement: Date are contained within the article.

Acknowledgments: We thank Qing-Hua Zhu for the useful discussions.

Conflicts of Interest: The authors declare no conflicts of interest.

Appendix A. Source Terms

$$\begin{aligned}\mathcal{S}_{ij,1}(\mathbf{x},\eta) = {} & 4\phi\partial_i\partial_j\phi + \partial_i\phi\partial_j\phi - \frac{\partial_i\phi'\partial_j\phi}{\mathcal{H}} - \frac{\partial_i\phi\partial_j\phi'}{\mathcal{H}} - \frac{\partial_i\phi'\partial_j\phi'}{\mathcal{H}^2} + \delta_{ij}\Big(-24\mathcal{H}\phi\phi' \\ & -2(\phi')^2 - 4\phi\phi'' - \frac{16}{3}\phi\Delta\phi - \frac{11}{3}\partial_b\phi\partial^b\phi + \frac{2}{3\mathcal{H}}\partial_b\phi'\partial^b\phi + \frac{1}{3\mathcal{H}^2}\partial_b\phi'\partial^b\phi'\Big)\,,\end{aligned} \tag{A1}$$

$$\begin{aligned}\mathcal{S}_{ij,2}(\mathbf{x},\eta) = {} & -h_{ij}''\phi - 2\mathcal{H}h_{ij}'\phi + 10\mathcal{H}h_{ij}\phi' + 3h_{ij}\phi'' - \phi\Delta h_{ij} - \frac{5}{3}h_{ij}\Delta\phi + h_j^b\partial_b\partial_i\phi \\ & + h_i^b\partial_b\partial_j\phi - 2\partial_b h_{ij}\partial^b\phi + \partial^b\phi\partial_i h_{jb} + \partial^b\phi\partial_j h_{ib} - \delta_{ij}\frac{2}{3}h^{bc}\partial_c\partial_b\phi\,,\end{aligned} \tag{A2}$$

$$\begin{aligned}\mathcal{S}_{ij,3}(\mathbf{x},\eta) = {} & -\frac{1}{2}h_i^{b'}h_{jb}' + \frac{1}{2}h^{bc}\partial_c\partial_b h_{ij} - \frac{1}{2}h^{bc}\partial_c\partial_i h_{jb} - \frac{1}{2}h^{bc}\partial_c\partial_j h_{ib} - \frac{1}{2}\partial_b h_{jc}\partial^c h_i^b \\ & + \frac{1}{2}\partial_c h_{jb}\partial^c h_i^b + \frac{1}{4}\partial_i h^{bc}\partial_j h_{bc} + \frac{1}{2}h^{bc}\partial_i\partial_j h_{bc} + \delta_{ij}\Big(\frac{5}{12}h_{bc}'h'^{bc} + \frac{1}{2}h^{bc}h_{bc}'' \\ & + \frac{4\mathcal{H}}{3}h^{bc}h_{bc}' - \frac{2}{3}h^{bc}\Delta h_{bc} + \frac{1}{3}\partial_c h_{bd}\partial^d h^{bc} - \frac{1}{2}\partial_d h_{bc}\partial^d h^{bc}\Big)\,,\end{aligned} \tag{A3}$$

where in Equations (A1)–(A3), we have defined $\partial_\eta\phi \equiv \phi'$. The source terms in momentum space are given by

$$
\begin{aligned}
S_{ij,1}(\mathbf{k},\eta) = -\int \frac{d^3p}{(2\pi)^{3/2}}\Bigg(&4p_ip_jT_\phi(ux)T_\phi(vx) + \big((k-p)_ip_j\big)\Bigg(T_\phi(ux)T_\phi(vx) - ux\frac{d}{d(ux)}T_\phi(ux)T_\phi(vx)\\
&-vxT_\phi(ux)\frac{d}{d(vx)}T_\phi(vx) - vux^2\frac{d}{d(ux)}T_\phi(ux)\frac{d}{d(vx)}T_\phi(vx)\Bigg) - \delta_{ij}\Bigg(-\frac{24vk^2}{x}T_\phi(ux)T'_\phi(vx)\\
&-2uvk^2T'_\phi(ux)T'_\phi(vx) - 4v^2k^2T_\phi(ux)T''_\phi(vx) + \frac{16v^2k^2}{3}T_\phi(ux)T_\phi(vx)\\
&+\frac{11k^2(1-u^2-v^2)}{6}T_\phi(ux)T_\phi(vx) - \frac{k^2(1-u^2-v^2)ux}{3}T'_\phi(ux)T_\phi(vx)\\
&-\frac{k^2(1-u^2-v^2)x^2uv}{6}T'_\phi(ux)T'_\phi(vx)\Bigg)\Bigg)\frac{4}{9}\zeta_{\mathbf{k}-\mathbf{p}}\zeta_{\mathbf{p}}\,,
\end{aligned}
\tag{A4}
$$

$$
\begin{aligned}
S_{ij,2}(\mathbf{k},\eta) = \int \frac{d^3p}{(2\pi)^{3/2}}\Big(&-\Big((k-p)^bp_i\Big)\varepsilon^\lambda_{jb}(\mathbf{p})T_\phi(ux)T_h(vx) - \Big((k-p)^bp_j\Big)\varepsilon^\lambda_{ib}(\mathbf{p})T_\phi(ux)T_h(vx)\\
&-((k-p)_b(k-p)_i)\varepsilon^{\lambda,b}_j(\mathbf{p})T_\phi(ux)T_h(vx) - \big((k-p)_b(k-p)_j\big)\varepsilon^{\lambda,b}_i(\mathbf{p})T_\phi(ux)T_h(vx)\\
&+\varepsilon^\lambda_{ij}(\mathbf{p})\Bigg(-v^2k^2T_\phi(ux)\frac{d^2}{d(vx)^2}T_h(vx) - \frac{2vk^2}{x}T_\phi(ux)\frac{d}{d(vx)}T_h(vx)\\
&+3u^2k^2\frac{d^2}{d(ux)^2}T_\phi(ux)T_h(vx) + v^2k^2T_\phi(ux)T_h(vx) + \frac{5u^2k^2}{3}T_\phi(ux)T_h(vx)\\
&+k^2\Big(1-v^2-u^2\Big)T_\phi(ux)T_h(vx) + \frac{10uk^2}{x}\frac{d}{d(ux)}T_\phi(ux)T_h(vx)\Bigg)\\
&+\delta_{ij}\varepsilon^{\lambda,bc}(\mathbf{p})(k-p)_b(k-p)_c\Bigg(\frac{2}{3}T_\phi(ux)T_h(vx)\Bigg)\Big)\frac{2}{3}\zeta_{\mathbf{k}-\mathbf{p}}\mathbf{h}^\lambda_{\mathbf{p}}\,,
\end{aligned}
\tag{A5}
$$

$$
\begin{aligned}
S_{ij,3}(\mathbf{k},\eta) = \int \frac{d^3p}{(2\pi)^{3/2}}\frac{1}{2}\Bigg(&\varepsilon^{\lambda_1,b}_i(\mathbf{k}-\mathbf{p})\varepsilon^{\lambda_2}_{jb}(\mathbf{p})\Bigg(-uvk^2\frac{d}{(ux)}T_h(ux)\frac{d}{(vx)}T_h(vx)\\
&-\frac{k^2(1-v^2-u^2)}{2}T_h(ux)T_h(vx)\Bigg) - \varepsilon^{\lambda_1,bc}(\mathbf{k}-\mathbf{p})\varepsilon^{\lambda_2}_{ij}(\mathbf{p})p_bp_cT_h(ux)T_h(vx)\\
&+\varepsilon^{\lambda_1,bc}(\mathbf{k}-\mathbf{p})\varepsilon^{\lambda_2}_{jb}(\mathbf{p})p_cp_iT_h(ux)T_h(vx) + \varepsilon^{\lambda_1,bc}(\mathbf{k}-\mathbf{p})\varepsilon^{\lambda_2}_{ib}(\mathbf{p})p_cp_jT_h(ux)T_h(vx)\\
&-\varepsilon^{\lambda_1,bc}(\mathbf{k}-\mathbf{p})\varepsilon^{\lambda_2}_{bc}(\mathbf{p})\Bigg(\frac{1}{2}(k-p)_ip_jT_h(ux)T_h(vx) + p_ip_jT_h(ux)T_h(vx)\Bigg)\\
&+\varepsilon^{\lambda_1}_{jc}(\mathbf{k}-\mathbf{p})\varepsilon^{\lambda_2,b}_i(\mathbf{p})(k-p)_bp^cT_h(ux)T_h(vx)\\
&+2\delta_{ij}\Bigg(\varepsilon^{\lambda_1}_{bc}(\mathbf{k}-\mathbf{p})\varepsilon^{\lambda_2,bc}(\mathbf{p})\Bigg(\frac{5uvk^2}{12}T'_h(ux)T'_h(vx) + \frac{v^2k^2}{2}T_h(ux)T''_h(vx)\\
&+\frac{4vk^2}{3x}T_h(ux)T'_h(vx) + \frac{2v^2k^2}{3}T_h(ux)T_h(vx) + \frac{k^2(1-u^2-v^2)}{4}T_h(ux)T_h(vx)\Bigg)\\
&-\frac{1}{3}\varepsilon^{\lambda_1}_{bd}(\mathbf{k}-\mathbf{p})\varepsilon^{\lambda_2,bc}(\mathbf{p})(k-p)_cp^dT_h(ux)T_h(vx)\Bigg)\Bigg)\mathbf{h}^{\lambda_1}_{\mathbf{k}-\mathbf{p}}\mathbf{h}^{\lambda_2}_{\mathbf{p}}\,.
\end{aligned}
\tag{A6}
$$

In Equations (A4)–(A6), we have defined $|\mathbf{k}-\mathbf{p}| = u|\mathbf{k}| = uk$ and $p = |\mathbf{p}| = vk$. The explicit expressions of polarization tensor $\varepsilon^{\lambda_1,ij}(\mathbf{p})$ are given in Appendix B. The first-order scalar and tensor perturbations in Equations (A4)–(A6) have been written as

$$
\psi(\eta,\mathbf{k}) = \phi(\eta,\mathbf{k}) = \frac{2}{3}\zeta_{\mathbf{k}}T_\phi(k\eta)\,,\; h^\lambda(\eta,\mathbf{k}) = \mathbf{h}^\lambda_{\mathbf{k}}T_h(k\eta)\,,
\tag{A7}
$$

where $\zeta_{\mathbf{k}}$ and $\mathbf{h}_{\mathbf{k}}$ are the primordial curvature and tensor perturbations, respectively. The transfer functions $T_\phi(k\eta)$ and $T_h(k\eta)$ in the RD era are given by [32]

$$T_\phi(x) = \frac{9}{x^2}\left(\frac{\sqrt{3}}{x}\sin\left(\frac{x}{\sqrt{3}}\right) - \cos\left(\frac{x}{\sqrt{3}}\right)\right),\ T_h = \frac{\sin x}{x}\,. \tag{A8}$$

Appendix B. Polarization Tensor

The polarization tensor is defined as

$$\varepsilon_{ij}^{\times}(\mathbf{k}) = \frac{1}{\sqrt{2}}\big(e_i(\mathbf{k})\bar{e}_j(\mathbf{k}) + \bar{e}_i(\mathbf{k})e_j(\mathbf{k})\big)\,, \tag{A9}$$

$$\varepsilon_{ij}^{+}(\mathbf{k}) = \frac{1}{\sqrt{2}}\big(e_i(\mathbf{k})e_j(\mathbf{k}) - \bar{e}_i(\mathbf{k})\bar{e}_j(\mathbf{k})\big)\,, \tag{A10}$$

where $(\mathbf{k}_i/|k|, e_i(\mathbf{k}), \bar{e}_i(\mathbf{k}))$ is the normalized bases in three-dimensional momentum space. We study the polarization tensor for a given coordinate system, namely,

$$\mathbf{k} = (0,0,k)\,,\ e_i(\mathbf{k}) = (1,0,0)\,,\ \bar{e}_i(\mathbf{k}) = (0,1,0)\,. \tag{A11}$$

Then, polarization tensors $\varepsilon_{ij}^{\lambda}(\mathbf{k}-\mathbf{p})$ and $\varepsilon_{ij}^{\lambda}(\mathbf{p})$ can be written as

$$\begin{aligned}
\varepsilon_{ij}^{\times}(\mathbf{k}-\mathbf{p}) &= \frac{1}{\sqrt{2}}\big(e_i(\mathbf{k}-\mathbf{p})\bar{e}_j(\mathbf{k}-\mathbf{p}) + \bar{e}_i(\mathbf{k}-\mathbf{p})e_j(\mathbf{k}-\mathbf{p})\big)\,,\\
\varepsilon_{ij}^{+}(\mathbf{k}-\mathbf{p}) &= \frac{1}{\sqrt{2}}\big(e_i(\mathbf{k}-\mathbf{p})e_j(\mathbf{k}-\mathbf{p}) - \bar{e}_i(\mathbf{k}-\mathbf{p})\bar{e}_j(\mathbf{k}-\mathbf{p})\big)\,,\\
\varepsilon_{ij}^{\times}(\mathbf{p}) &= \frac{1}{\sqrt{2}}\big(e_i(\mathbf{p})\bar{e}_j(\mathbf{p}) + \bar{e}_i(\mathbf{p})e_j(\mathbf{p})\big)\,,\\
\varepsilon_{ij}^{+}(\mathbf{p}) &= \frac{1}{\sqrt{2}}\big(e_i(\mathbf{p})e_j(\mathbf{p}) - \bar{e}_i(\mathbf{p})\bar{e}_j(\mathbf{p})\big)\,,
\end{aligned} \tag{A12}$$

where

$$\begin{aligned}
\mathbf{k}-\mathbf{p} &= k\left(-\sqrt{v^2 - \frac{1}{4}(-u^2+v^2+1)^2}, 0, \frac{1}{2}\Big(u^2 - v^2 + 1\Big)\right),\\
e_i(\mathbf{k}-\mathbf{p}) &= \left(\frac{u^2-v^2+1}{2u}, 0, \frac{\sqrt{-u^4+2u^2v^2+2u^2-v^4+2v^2-1}}{2u}\right),\\
\bar{e}_i(\mathbf{k}-\mathbf{p}) &= (0,1,0)\,,
\end{aligned} \tag{A13}$$

$$\begin{aligned}
\mathbf{p} &= k\left(\sqrt{v^2 - \frac{1}{4}(-u^2+v^2+1)^2}, 0, \frac{1}{2}\Big(-u^2 + v^2 + 1\Big)\right),\\
e_i(\mathbf{p}) &= \left(-\frac{-u^2+v^2+1}{2v}, 0, \frac{\sqrt{-u^4+2u^2(v^2+1)-(v^2-1)^2}}{2v}\right),\\
\bar{e}_i(\mathbf{p}) &= (0,1,0)\,.
\end{aligned} \tag{A14}$$

Appendix C. Four-Point Function

$$\begin{aligned}
\Big\langle \zeta_{\mathbf{k}-\mathbf{p}}\zeta_{\mathbf{p}}\zeta_{\mathbf{k}'-\mathbf{p}'}\zeta_{\mathbf{p}'}\Big\rangle &= \Big\langle \zeta_{\mathbf{k}-\mathbf{p}}\zeta_{\mathbf{k}'-\mathbf{p}'}\Big\rangle\Big\langle \zeta_{\mathbf{p}}\zeta_{\mathbf{p}'}\Big\rangle + \Big\langle \zeta_{\mathbf{k}-\mathbf{p}}\zeta_{\mathbf{p}'}\Big\rangle\Big\langle \zeta_{\mathbf{p}}\zeta_{\mathbf{k}'-\mathbf{p}'}\Big\rangle\\
&= \delta(\mathbf{k}+\mathbf{k}')\frac{(2\pi^2)^2}{p^3|\mathbf{k}-\mathbf{p}|^3}\big(\delta(\mathbf{p}+\mathbf{p}') + \delta(\mathbf{k}'-\mathbf{p}'+\mathbf{p})\big)\mathcal{P}_\zeta(|\mathbf{k}-\mathbf{p}|)\mathcal{P}_\zeta(p)\,,
\end{aligned} \tag{A15}$$

$$\begin{aligned}\langle \zeta_{\mathbf{k}-\mathbf{p}} \mathbf{h}_{\mathbf{p}}^{\lambda_1} \zeta_{\mathbf{k}'-\mathbf{p}'} \mathbf{h}_{\mathbf{p}'}^{\lambda_1'} \rangle =& \langle \zeta_{\mathbf{k}-\mathbf{p}} \zeta_{\mathbf{k}'-\mathbf{p}'} \rangle \langle \mathbf{h}_{\mathbf{p}}^{\lambda_1} \mathbf{h}_{\mathbf{p}'}^{\lambda_1'} \rangle \\ =& \delta(\mathbf{k}+\mathbf{k}') \delta^{\lambda_1 \lambda_1'} \frac{(2\pi^2)^2}{p^3 |\mathbf{k}-\mathbf{p}|^3} \delta(\mathbf{p}+\mathbf{p}') \mathcal{P}_\zeta(|\mathbf{k}-\mathbf{p}|) \mathcal{P}_h(p) \,, \end{aligned} \tag{A16}$$

$$\begin{aligned}\langle \mathbf{h}_{\mathbf{k}-\mathbf{p}}^{\lambda_1} \mathbf{h}_{\mathbf{p}}^{\lambda_2} \mathbf{h}_{\mathbf{k}'-\mathbf{p}'}^{\lambda_1'} \mathbf{h}_{\mathbf{p}'}^{\lambda_2'} \rangle =& \delta(\mathbf{k}+\mathbf{k}') \frac{(2\pi^2)^2}{p^3 |\mathbf{k}-\mathbf{p}|^3} \Big(\delta^{\lambda_1 \lambda_1'} \delta^{\lambda_2 \lambda_2'} \delta(\mathbf{p}+\mathbf{p}') + \delta^{\lambda_1 \lambda_1'} \delta^{\lambda_2 \lambda_1'} \delta(\mathbf{k}'-\mathbf{p}'+\mathbf{p}) \Big) \\ & \times \mathcal{P}_h(|\mathbf{k}-\mathbf{p}|) \mathcal{P}_h(p) \,. \end{aligned} \tag{A17}$$

References

1. Aghanim, N.; Akrami, Y.; Ashdown, M.; Aumont, J.; Baccigalupi, C.; Ballardini, M.; Banday, A.J.; Barreiro, R.B.; Bartolo, N.; Basak, S.; et al. Planck 2018 results. VI. Cosmological parameters. *Astron. Astrophys.* **2020**, *641*, A6; Erratum in *Astron. Astrophys.* **2021**, *652*, C4. [CrossRef]
2. Malik, K.A.; Wands, D. Cosmological perturbations. *Phys. Rep.* **2009**, *475*, 1–51. [CrossRef]
3. Mukhanov, V.F.; Feldman, H.A.; Brandenberger, R.H. Theory of cosmological perturbations. Part 1. Classical perturbations. Part 2. Quantum theory of perturbations. Part 3. Extensions. *Phys. Rep.* **1992**, *215*, 203–333. [CrossRef]
4. Kodama, H.; Sasaki, M. Cosmological Perturbation Theory. *Prog. Theor. Phys. Suppl.* **1984**, *78*, 1–166. [CrossRef]
5. Mollerach, S.; Harari, D.; Matarrese, S. CMB polarization from secondary vector and tensor modes. *Phys. Rev. D* **2004**, *69*, 063002. [CrossRef]
6. Baumann, D.; Steinhardt, P.J.; Takahashi, K.; Ichiki, K. Gravitational Wave Spectrum Induced by Primordial Scalar Perturbations. *Phys. Rev. D* **2007**, *76*, 084019. [CrossRef]
7. Kohri, K.; Terada, T. Semianalytic calculation of gravitational wave spectrum nonlinearly induced from primordial curvature perturbations. *Phys. Rev. D* **2018**, *97*, 123532. [CrossRef]
8. Domènech, G. Scalar Induced Gravitational Waves Review. *Universe* **2021**, *7*, 398. [CrossRef]
9. Chang, Z.; Kuang, Y.T.; Zhang, X.; Zhou, J.Z. Primordial black holes and third order scalar induced gravitational waves. *Chin. Phys. C* **2023**, *47*, 055104. [CrossRef]
10. Romero-Rodriguez, A.; Martinez, M.; Pujolàs, O.; Sakellariadou, M.; Vaskonen, V. Search for a Scalar Induced Stochastic Gravitational Wave Background in the Third LIGO-Virgo Observing Run. *Phys. Rev. Lett.* **2022**, *128*, 051301. [CrossRef]
11. Saito, R.; Yokoyama, J. Gravitational wave background as a probe of the primordial black hole abundance. *Phys. Rev. Lett.* **2009**, *102*, 161101; Erratum in *Phys. Rev. Lett.* **2011**, *107*, 069901. [CrossRef] [PubMed]
12. Wang, S.; Terada, T.; Kohri, K. Prospective constraints on the primordial black hole abundance from the stochastic gravitational-wave backgrounds produced by coalescing events and curvature perturbations. *Phys. Rev. D* **2019**, *99*, 103531; Erratum in *Phys. Rev. D* **2020**, *101*, 069901. [CrossRef]
13. Inomata, K.; Nakama, T. Gravitational waves induced by scalar perturbations as probes of the small-scale primordial spectrum. *Phys. Rev. D* **2019**, *99*, 043511. [CrossRef]
14. Barausse, E.; Berti, E.; Hertog, T.; Hughes, S.A.; Jetzer, P.; Pani, P.; Sotiriou, T.P.; Tamanini, N.; Witek, H.; Yagi, K.; et al. Prospects for Fundamental Physics with LISA. *Gen. Relativ. Gravit.* **2020**, *52*, 81. [CrossRef]
15. Bartolo, N.; De Luca, V.; Franciolini, G.; Lewis, A.; Peloso, M.; Riotto, A. Primordial Black Hole Dark Matter: LISA Serendipity. *Phys. Rev. Lett.* **2019**, *122*, 211301. [CrossRef] [PubMed]
16. Cai, R.g.; Pi, S.; Sasaki, M. Gravitational Waves Induced by non-Gaussian Scalar Perturbations. *Phys. Rev. Lett.* **2019**, *122*, 201101. [CrossRef]
17. Chang, Z.; Zhang, X.; Zhou, J.Z. Gravitational waves from primordial scalar and tensor perturbations. *Phys. Rev. D* **2023**, *107*, 063510. [CrossRef]
18. Inomata, K.; Kawasaki, M.; Mukaida, K.; Tada, Y.; Yanagida, T.T. Inflationary primordial black holes for the LIGO gravitational wave events and pulsar timing array experiments. *Phys. Rev. D* **2017**, *95*, 123510. [CrossRef]
19. Papanikolaou, T.; Vennin, V.; Langlois, D. Gravitational waves from a universe filled with primordial black holes. *J. Cosmol. Astropart. Phys.* **2021**, *3*, 053. [CrossRef]
20. Zhou, Z.; Jiang, J.; Cai, Y.F.; Sasaki, M.; Pi, S. Primordial black holes and gravitational waves from resonant amplification during inflation. *Phys. Rev. D* **2020**, *102*, 103527. [CrossRef]
21. Domènech, G.; Pi, S.; Sasaki, M. Induced gravitational waves as a probe of thermal history of the universe. *J. Cosmol. Astropart. Phys.* **2020**, *8*, 017. [CrossRef]
22. Cai, R.G.; Guo, Z.K.; Liu, J.; Liu, L.; Yang, X.Y. Primordial black holes and gravitational waves from parametric amplification of curvature perturbations. *J. Cosmol. Astropart. Phys.* **2020**, *6*, 013. [CrossRef]
23. Cai, R.G.; Pi, S.; Wang, S.J.; Yang, X.Y. Pulsar Timing Array Constraints on the Induced Gravitational Waves. *J. Cosmol. Astropart. Phys.* **2019**, *10*, 059. [CrossRef]
24. Yuan, C.; Chen, Z.C.; Huang, Q.G. Probing primordial–black-hole dark matter with scalar induced gravitational waves. *Phys. Rev. D* **2019**, *100*, 081301. [CrossRef]

25. Bartolo, N.; Domcke, V.; Figueroa, D.G.; García-Bellido, J.; Peloso, M.; Pieroni, M.; Ricciardone, A.; Sakellariadou, M.; Sorbo, L.; Tasinato, G. Probing non-Gaussian Stochastic Gravitational Wave Backgrounds with LISA. *J. Cosmol. Astropart. Phys.* **2018**, *11*, 034. [CrossRef]
26. Alabidi, L.; Kohri, K.; Sasaki, M.; Sendouda, Y. Observable induced gravitational waves from an early matter phase. *J. Cosmol. Astropart. Phys.* **2013**, *5*, 033. [CrossRef]
27. Zhang, X.; Zhou, J.Z.; Chang, Z. Impact of the free-streaming neutrinos to the second order induced gravitational waves. *Eur. Phys. J. C* **2022**, *82*, 781. [CrossRef]
28. Gong, J.O. Analytic Integral Solutions for Induced Gravitational Waves. *Astrophys. J.* **2022**, *925*, 102. [CrossRef]
29. Zhou, J.Z.; Zhang, X.; Zhu, Q.H.; Chang, Z. The third order scalar induced gravitational waves. *J. Cosmol. Astropart. Phys.* **2022**, *5*, 013. [CrossRef]
30. Arun, K.G.; Belgacem, E.; Benkel, R.; Bernard, L.; Berti, E.; Bertone, G.; Besancon, M.; Blas, D.; Böhmer, C.G.; Brito, R.; et al. New horizons for fundamental physics with LISA. *Living Rev. Relativ.* **2022**, *25*, 4. [CrossRef]
31. Zhao, Z.C.; Wang, S. Bayesian implications for the primordial black holes from NANOGrav's pulsar-timing data by using the scalar induced gravitational waves. *Universe* **2023**, *9*, 157. [CrossRef]
32. Inomata, K. Analytic solutions of scalar perturbations induced by scalar perturbations. *J. Cosmol. Astropart. Phys.* **2021**, *3*, 013. [CrossRef]
33. Carrilho, P.; Malik, K.A. Vector and tensor contributions to the curvature perturbation at second order. *J. Cosmol. Astropart. Phys.* **2016**, *2*, 021. [CrossRef]
34. Zhang, Y.; Qin, F.; Wang, B. Second-order cosmological perturbations. II. Produced by scalar-tensor and tensor-tensor couplings. *Phys. Rev. D* **2017**, *96*, 103523. [CrossRef]
35. Nakama, T.; Suyama, T. Primordial black holes as a novel probe of primordial gravitational waves. II: Detailed analysis. *Phys. Rev. D* **2016**, *94*, 043507. [CrossRef]
36. Nakama, T.; Suyama, T. Primordial black holes as a novel probe of primordial gravitational waves. *Phys. Rev. D* **2015**, *92*, 121304. [CrossRef]
37. Bari, P.; Ricciardone, A.; Bartolo, N.; Bertacca, D.; Matarrese, S. Signatures of Primordial Gravitational Waves on the Large-Scale Structure of the Universe. *Phys. Rev. Lett.* **2022**, *129*, 091301. [CrossRef]
38. Cho, I.; Gong, J.O.; Oh, S.H. Second-order effective energy-momentum tensor of gravitational scalar perturbations with perfect fluid. *Phys. Rev. D* **2020**, *102*, 043531. [CrossRef]
39. Saga, S. The Vector Mode in the Second-order Cosmological Perturbation Theory. Ph.D. Thesis, Nagoya University, Nagoya, Japan, 2017. [CrossRef]
40. Lu, T.H.C.; Ananda, K.; Clarkson, C. Vector modes generated by primordial density fluctuations. *Phys. Rev. D* **2008**, *77*, 043523. [CrossRef]
41. Lu, T.H.C.; Ananda, K.; Clarkson, C.; Maartens, R. The cosmological background of vector modes. *J. Cosmol. Astropart. Phys.* **2009**, *2*, 023. [CrossRef]
42. Smith, R.E.; Sheth, R.K.; Scoccimarro, R. An analytic model for the bispectrum of galaxies in redshift space. *Phys. Rev. D* **2008**, *78*, 023523. [CrossRef]
43. Acquaviva, V.; Bartolo, N.; Matarrese, S.; Riotto, A. Second order cosmological perturbations from inflation. *Nucl. Phys. B* **2003**, *667*, 119–148. [CrossRef]
44. Kamionkowski, M.; Kosowsky, A.; Stebbins, A. A Probe of primordial gravity waves and vorticity. *Phys. Rev. Lett.* **1997**, *78*, 2058–2061. [CrossRef]
45. Durrer, R. Light deflection in perturbed Friedmann universes. *Phys. Rev. Lett.* **1994**, *72*, 3301–3304. [CrossRef] [PubMed]
46. Yamauchi, D.; Namikawa, T.; Taruya, A. Weak lensing generated by vector perturbations and detectability of cosmic strings. *J. Cosmol. Astropart. Phys.* **2012**, *10*, 030. [CrossRef]
47. Saga, S.; Yamauchi, D.; Ichiki, K. Weak lensing induced by second-order vector mode. *Phys. Rev. D* **2015**, *92*, 063533. [CrossRef]
48. Chang, Z.; Zhang, X.; Zhou, J.Z. The cosmological vector modes from a monochromatic primordial power spectrum. *J. Cosmol. Astropart. Phys.* **2022**, *10*, 084. [CrossRef]
49. Akrami, Y.; Arroja, F.; Ashdown, M.; Aumont, J.; Baccigalupi, C.; Ballardini, M.; Banday, A.J.; Barreiro, R.B.; Bartolo, N.; Basak, S.; et al. Planck 2018 results. X. Constraints on inflation. *Astron. Astrophys.* **2020**, *641*, A10. [CrossRef]
50. Bringmann, T.; Scott, P.; Akrami, Y. Improved constraints on the primordial power spectrum at small scales from ultracompact minihalos. *Phys. Rev. D* **2012**, *85*, 125027. [CrossRef]
51. Ananda, K.N.; Clarkson, C.; Wands, D. The Cosmological gravitational wave background from primordial density perturbations. *Phys. Rev. D* **2007**, *75*, 123518. [CrossRef]
52. Alabidi, L.; Kohri, K.; Sasaki, M.; Sendouda, Y. Observable Spectra of Induced Gravitational Waves from Inflation. *J. Cosmol. Astropart. Phys.* **2012**, *9*, 017. [CrossRef]
53. Bugaev, E.; Klimai, P. Induced gravitational wave background and primordial black holes. *Phys. Rev. D* **2010**, *81*, 023517. [CrossRef]
54. Inomata, K.; Kawasaki, M.; Mukaida, K.; Yanagida, T.T. Double inflation as a single origin of primordial black holes for all dark matter and LIGO observations. *Phys. Rev. D* **2018**, *97*, 043514. [CrossRef]

55. Garcia-Bellido, J.; Peloso, M.; Unal, C. Gravitational Wave signatures of inflationary models from Primordial Black Hole Dark Matter. *J. Cosmol. Astropart. Phys.* **2017**, *9*, 013. [CrossRef]
56. Sasaki, M.; Suyama, T.; Tanaka, T.; Yokoyama, S. Primordial black holes—perspectives in gravitational wave astronomy. *Class. Quant. Grav.* **2018**, *35*, 063001. [CrossRef]
57. Kobayashi, T.; Yamaguchi, M.; Yokoyama, J. Generalized G-inflation: Inflation with the most general second-order field equations. *Prog. Theor. Phys.* **2011**, *126*, 511–529. [CrossRef]
58. Gorji, M.A.; Sasaki, M. Primordial-tensor-induced stochastic gravitational waves. *Phys. Lett. B* **2023**, *846*, 138236. [CrossRef]
59. Chen, C.; Ota, A.; Zhu, H.Y.; Zhu, Y. Missing one-loop contributions in secondary gravitational waves. *arXiv* **2022**, arXiv:2210.17176.
60. Bari, P.; Bartolo, N.; Domènech, G.; Matarrese, S. Gravitational waves induced by scalar-tensor mixing. *arXiv* **2023**, arXiv:2307.05404.
61. Picard, R.; Malik, K.A. Induced gravitational waves: The effect of first order tensor perturbations. *arXiv* **2023**, arXiv:2311.14513.
62. Cho, I.; Gong, J.O.; Oh, S.H. Second-order energy-momentum tensor of a scalar field. *Phys. Rev. D* **2022**, *106*, 084027. [CrossRef]
63. Pitrou, C.; Roy, X.; Umeh, O. xPand: An algorithm for perturbing homogeneous cosmologies. *Class. Quant. Grav.* **2013**, *30*, 165002. [CrossRef]
64. Bartolo, N.; Komatsu, E.; Matarrese, S.; Riotto, A. Non-Gaussianity from inflation: Theory and observations. *Phys. Rep.* **2004**, *402*, 103–266. [CrossRef]
65. Bartolo, N.; Matarrese, S.; Riotto, A. Gauge-invariant temperature anisotropies and primordial non-Gaussianity. *Phys. Rev. Lett.* **2004**, *93*, 231301. [CrossRef]
66. Young, S.; Byrnes, C.T. Signatures of non-gaussianity in the isocurvature modes of primordial black hole dark matter. *J. Cosmol. Astropart. Phys.* **2015**, *4*, 034. [CrossRef]
67. Yu, Y.H.; Wang, S. Primordial Gravitational Waves Assisted by Cosmological Scalar Perturbations. *arXiv* **2023**, arXiv:2303.03897.
68. De Luca, V.; Kehagias, A.; Riotto, A. How well do we know the primordial black hole abundance: The crucial role of nonlinearities when approaching the horizon. *Phys. Rev. D* **2023**, *108*, 063531. [CrossRef]